Monitoring of tidal influences on the saline interface using resistivity traversing and cross-borehole resistivity tomography

F.J. Morrow [a,1], M.R. Ingham [b,*], J.A. McConchie [a,1]

[a] School of Geography, Environment & Earth Science, Victoria University of Wellington, PO Box 600, Wellington, New Zealand
[b] School of Chemical & Physical Sciences, Victoria University of Wellington, PO Box 600, Wellington, New Zealand

S U M M A R Y

Tidal influences on the saline interface of a shallow unconfined aquifer have been investigated by using both dc resistivity traversing and cross-borehole resistivity tomography (CRT). Variations in bulk resistivity structure obtained through resistivity traversing provide a clear general picture of the structure of the saline interface and its mixing zone. On all three resistivity traverses there are also indications that a small degree of mixing of saline and fresh water is occurring ahead of the main saline boundary. For one of the traverses much more detail of variations in resistivity structure is provided by CRT utilising three 10 m long electrode strings installed at 10 m separation. CRT images of the saline mixing zone do not reveal any significant difference between low and high tide for tidal ranges of about 2 m, but for a tidal range of approximately twice this clearly show effects due to both increased wave run-up and tidal head. Correlation of the bulk resistivity with fluid resistivity values measured in parallel bores suggests that although there is no apparent widening of the mixing zone during the tidal cycle significant variations in salinity do occur which can be envisaged in terms of the horizontal movement of near vertical salinity contours.

© 2010 Elsevier B.V. All rights reserved.

1. Introduction

Coastal aquifers form major sources of water throughout the world (International Association of Hydrologists, 2003). For example, in New Zealand they supply over 50% of all groundwater (White, 2001). Such resources are extremely vulnerable to salinisation from saltwater intrusion. Nevertheless, despite the critical role played by coastal aquifers as global groundwater resources, the nature and dynamics of the saline interface are not well understood. In coastal aquifers the position of the saline interface represents an equilibrium between freshwater and seawater potentiometric heads. The saline interface is not a sharp boundary and is fixed in neither time nor space. It is best considered as a zone of mixing which varies in response to anything that changes the difference between freshwater and seawater heads. This may include tidal action as well as variations in groundwater flow, increased groundwater extraction, and, potentially, changes in sea level. Although little is known about sea level rise as a potential cause of saline intrusion, the focus of research in this area is starting to shift because of a wider acceptance of climate change, and the potential for sea level rise. However, to predict the conse-

quences of any rise in sea level, the controls on, and dynamics of, the saline interface under natural conditions must first be understood.

Sea water, with a resistivity $\sim$0.3 Ωm, of is one of the most electrically conductive substances found naturally at the earth's surface. In comparison fresh water has a resistivity of $\sim$10–100 Ωm. The change from fresh to saline water can therefore be readily determined using electrical resistivity techniques. Indeed, the clear contrast between the bulk resistivity of sand saturated with fresh or saline water makes the use of electrical techniques an obvious choice for studying the saline interface (Acworth and Dasey, 2003). Many examples exist of studies where electrical measurements have been employed in such investigations. These include the use of dc resistivity soundings (e.g. Ebraheem et al., 1997; Choudhury et al., 2001), resistivity traversing (e.g. Wilson et al., 2006; Batayneh, 2006; Koukadaki et al., 2007), and electromagnetic measurements (e.g. Goldman et al., 1991; Albouy et al., 2001; Duque et al., 2008).

In this paper we report the results of a study which uses both resistivity traversing and the less commonly employed cross-borehole resistivity tomography (CRT) to investigate the location of and dynamics of the saline interface in an unconfined coastal aquifer. CRT (Daniels, 1977; Shima, 1992) utilises measurements made between strings of electrodes in boreholes to derive detailed models of the electrical resistivity structure between the boreholes. CRT

has been used in several studies aimed at measuring and monitoring subsurface flow (e.g. Slater et al., 2000; Looms et al., 2008) and in a previous study of the salinity structure beneath a beach-face (Turner and Acworth, 2004). A closely related technique, that of borehole to surface resistivity measurements, has also been used by Bauer et al. (2006) in a deltaic environment. In studies of the saline interface CRT holds the promise of being able to provide more detailed images of the resistivity structure than can be obtained from surface resistivity measurements which suffer a loss of resolution with depth. Time lapse measurements may also enable temporal variations of the saline interface to be observed and lead to an improved understanding of the diffusive processes taking place at the boundary. Temporal variations of interest include not only those due to wave and tidal action but, ultimately, those that may possibly arise from sea level changes.

The present study therefore aims to assess the ability of a combination of surface and cross-borehole resistivity measurements to address four fundamental issues: (1) to locate the seaward boundary of a shallow unconfined aquifer; (2) to determine the character and dynamics of the saline interface; (3) to examine the response of the saline interface to tidal fluctuations and other stimuli; and (4) to analyse the potential for landward movement of the saline interface as a result of any sea level rise.

2. Location and hydrogeology of the study area

The study area, the Kapiti Coast in the south-west of the lower North Island of New Zealand (Fig. 1), lies on the narrow (approximately 10 km wide) coastal plain to the north-west of the Tararua Ranges. The mean annual rainfall (1035 mm at Paraparaumu)

shows a marked decrease from south-east to north-west, as well as a degree of seasonality. The driest month (February) has about 50 mm of rainfall compared to over 100 mm per month in June and July. The Kapiti Coast is one of the fastest growing areas of New Zealand in terms of population and development and this has created an increasing demand for water resources and led to a growing number of water resource management issues resulting from a combination of the local scarcity of water suitable for human consumption, variability in rainfall from year to year, growing population, and high per capita water usage.

Until recently, the Waikanae River (Fig. 1) was the only source of potable water. Although the river flows 365 days per year, the substantially reduced flow during a prolonged dry period during the summer of 2002–2003 led to the imposition of severe water restrictions. To supplement water supplies during dry periods, in 2004 the local council (Kapiti Coast District Council – KCDC) installed a borefield to draw water from deep (60–80 m) aquifers. In addition to these deep bores, there are between 3000 and 4000 shallow bores in the area, most of which are less than 6 m deep and are used for garden irrigation. The amount of groundwater they use is unknown (Wellington Regional Council, 2000; URS, 2004a) but has been estimated as peaking during the summer months at approximately 5–6000 m³/day (Jones and Gyopari 2005). Cumulatively, these abstractions from the groundwater system have the potential to effect the dynamic equilibrium that defines the location and structure of the saline interface. The study area therefore represents an excellent example of coastal aquifers which are being placed under increasing demand.

Under the surface of the coastal plain lie three known aquifers (Wellington Regional Council, 1994) contained within six strati-
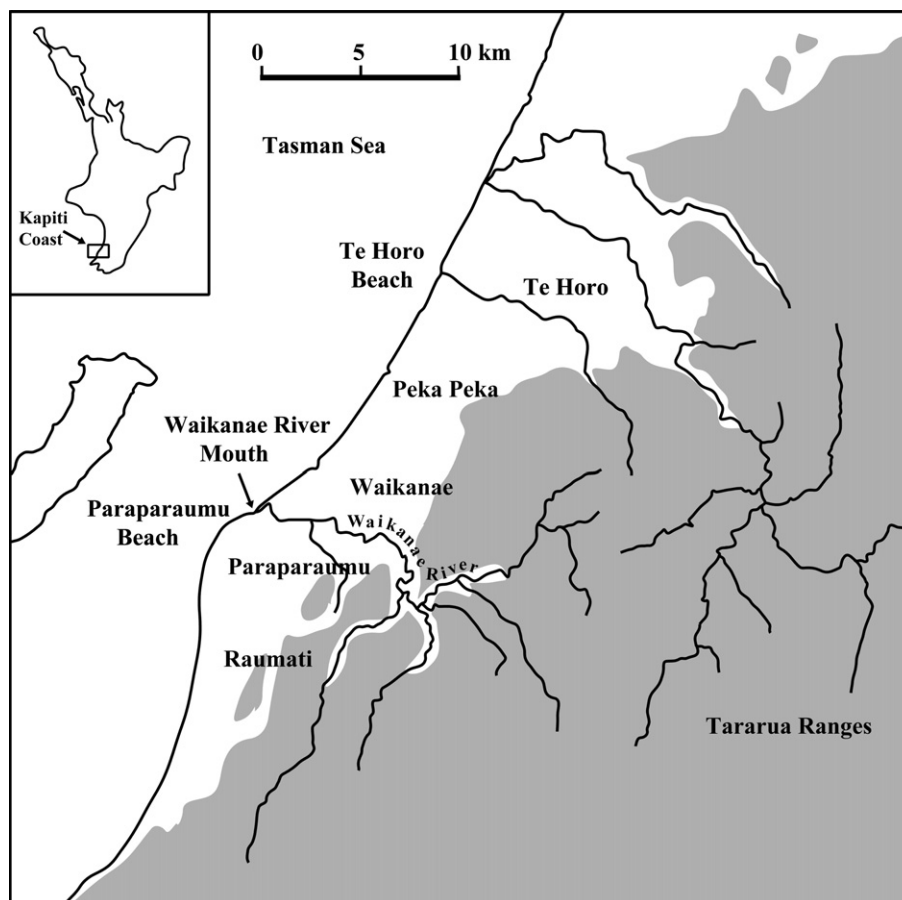

Fig. 1. The Kapiti Coast, North Island of New Zealand, showing main rivers/watercourses and locations mentioned in the text. Shading shows land over 100 m above sea level.

graphic units (URS, 2003). The six units all have a similar sequence, are up to 20 m thick and, as do similar units on the west coast of the North Island of New Zealand, reflect a Milankovitch-frequency sedimentary cycle of 100,000 years. The stratigraphic units are not horizontal but dip towards the coast. Groundwater flows through each of the six units, with the preferential flow path being towards the northwest through layers of gravel and sand. Although layers of silt and clay within the units generally restrict large vertical movement of water, URS (2003) suggested that there is an upward hydraulic gradient from the deeper aquifers to the shallower units in coastal areas, and a downward gradient in the inland areas. The upward gradient is demonstrated by a head difference of 600 mm between a deep (74 m) and a shallow well (21 m) at a location on the north bank of the Waikanae River some 1 km from the coast. It is also made evident by the emergence of springs that maintain flow in the Waimea Stream (Fig. 2). The downward gradient is apparent where the Waikanae River loses between 300 and 350 l/s (Welch, 2004; Harkness, 2004; Jones and Gyopari, 2005) to the groundwater system over a 2 km stretch of the river some 3–4 km inland from the river mouth. Groundwater salinity generally decreases with distance from the coast. Moreover, at deeper levels (⩾40 m) the iron and manganese content tends to be higher indicating that the deeper water is older than the shallow water.

The shallow aquifer system consists of the upper two stratigraphic units and is unconfined in westward-thickening, fine sand-rich sediment. It is generally about 20 m thick, but thickens to almost 30 m at the present coastline. The shallow system is principally recharged by rainfall (approximately 65%, Jones and Gyopari (2005)) and, in the eastern part of the coastal plain, by leakage through the bed of the Waikanae River. Other sources of recharge include lateral inflow from older terrace sediments to the east, and, close to the coast, upward leakage from deeper aquifers. Water levels in the shallow unconfined aquifer system are monitored by the Wellington Regional Council and show a seasonal variation of up to 1.5 m. Large increases in groundwater level measured by electronic data loggers collate strongly with significant rainfall events, indicating that the shallow aquifers respond quickly to rainfall recharge (Jones and Gyopari, 2005). Stratigraphic cross sections presented by Osborne (2006), combined with the bore log for a deep well located on the northern side of the Waikanae River mouth indicate that the sediment at the coastline is predominantly sand to at least 15 m depth. This was deposited during the marine transgression at the end of the last glacial and the following coastal progradation, as well as during intermediate stages of low activity. This group of sediments starts at the base of a postglacial sea cliff (Fig. 2) and thickens towards the coast. The saline interface of the shallow aquifer system lies within this coastal wedge of sand deposits.

Until recently research focussing on the groundwater of the Kapiti Coast, and in particular the Waikanae Groundwater Zone, covering the region within approx 3 km of the coast from Raumati to Peka Peka (Fig. 1), has primarily been to provide an overview of the hydrology and hydrogeology of the area (Johannesson and Rapley, 1961; Reynolds, 1992; Wellington Regional Council, 1992, 1994). Large scale investigations associated with the establishment of the new borefield were completed in 2003 and 2004 (URS, 2003, 2004a, 2004b). Jones and Gyopari (2005) investigated the shallow groundwater system, with an emphasis on the sustainability of the water resource and developed a numerical groundwater model to specifically assess the impact of extractions on the Waikanae River and wetlands. Cozens (2003) and Ingham et al. (2006) reported the use of electrical resistivity methods to conclude that the Waikanae River and shallow groundwater system were hydraulically connected and that there was limited saline intrusion into the system. Bore monitoring and concurrent stream gaugings were carried out by Welch (2004). Ruehe (2004) used a water balance model to determine groundwater recharge from precipitation, while Osborne (2006) characterised the movement of groundwater and its relationship with the Waikanae River.

Previous research into the saline interface further north on the Kapiti Coast has been reported by Wilson (2003) and Wilson et al. (2006), who used resistivity traversing to map the extent of saline intrusion in the unconfined aquifer beneath Te Horo Beach township (Fig. 1). However, notwithstanding the limited study by Cozens (2003), using similar techniques, there has been no such study of the saline interface in the Paraparaumu/Waikanae area which, because of the large number of bores, is potentially threatened by the possibility of saline intrusion.

Fig. 2. Waikanae and Paraparaumu Beach area on the Kapiti Coast showing geomorphic features and the locations of the three resistivity traverses.

3. Resistivity traverses

To locate the saline interface of the unconfined shallow aquifer, three resistivity traverses were measured on Paraparaumu Beach to the south of the Waikanae River mouth (Fig. 2). The traverses were measured in the manner described by Wilson et al. (2006) and Ingham et al. (2006) using an ABEM SAS 300C resistivity meter and a manual electrode switching system. Measurements were made using the Wenner array with equally spaced electrodes at a minimum spacing of 5 m, and a maximum spacing of either 55 or 60 m. Traverse 1 was approximately 400 m south of the Waikanae River mouth and just over 160 m in length. Traverses 2 and 3 were 400 m and 800 m south of Traverse 1 and of lengths 150 and 200 m respectively. The slope of the beach averages 2° and continues into the sea at this rate for at least 300 m, however at their south-east end all three traverses passed up and over coastal dunes of approximately 4 m in height. On all three traverses topography was measured using a Sokkia Electronic Distance Meter (EDM) and was subsequently taken into account when modelling the resistivity data. The data from each traverse were inverted using the Res2dinv software based on the smoothness-constrained least-squares method of de Groot-Hedlin and Constable (1990) and Sasaki (1992).

The resulting two-dimensional resistivity model for Traverse 1 is shown in Fig. 3a and fits the data with a root mean square (rms) error of 2.9%. The derived model clearly shows that a significant resistivity boundary occurs just inland (SE) of the maximum high tide mark, close to the base of the dunes. Over a distance of about 10 m the resistivity rises by a factor of 10. The shape of this transition zone is very similar to that of the sharp saline boundary given by simple theoretical models such as the Ghyben–Herzberg model which predict that under hydrostatic conditions the depth of the saline boundary at any point is approximately 40 times the freshwater head. Beneath the beach a resistivity of less than about 3 Ωm persists to about 20 m depth – comparable to the expected thickness of the unconfined aquifer.

Measurements on Traverse 1 were initially made at low tide. Measurements were subsequently repeated at high tide. The derived resistivity model from the high tide data showed no significant difference from that shown in Fig. 3a, indicating that either the saline interface at this location is unaffected by tidal fluctuations or any effects are too small to be resolved at this scale. As a result measurements on both Traverses 2 and 3 were made only at low tide. Derived resistivity models for these traverses are shown in Fig. 3b and c respectively and have rms errors of 1.9 and 3.3% respectively.

It is apparent from the models shown in Fig. 3 that there are both similarities and significant differences in the resistivity structure beneath the 3 traverses. In general the following observations can be made:

(i) A transition zone (3.2–32 Ωm, shown in green colours in Fig. 3) from low resistivity to high resistivity occurs close to the base of the coastal dunes on all three traverses.
(ii) Resistivity values beneath the coastal dunes are generally indicative of either dry or fresh water saturated sand. However, on each of the three traverses there are indications (resistivity in the range of 30–50 Ωm) that penetration or mixing of saline water has occurred to at least some degree. These values are less than the 50–100 Ωm quoted for freshwater in a similar geological environment by Wilson et al. (2006), citing White (1985). Such values were argued by Wilson et al. (2006) to be typical of 1–2% of saline mixing.
(iii) With increasing distance from the Waikanae River mouth there is a distinct decrease in the thickness of the near-surface very low resistivity zone (<3 Ωm) beneath the beach.

(iv) The observed deeper resistivity of ∼10 Ωm beneath Traverse 1 is replaced beneath Traverse 2 by a tongue of higher resistivity (10–30 Ωm) extending seaward from beneath the dunes. Beneath Traverse 3 the deeper resistivity is higher still (30–50 Ωm). These values are all lower than would be expected for fresh water saturated sands. For Traverses 2 and 3 any detail in the resistivity structure at depths in the range 5–15 m is largely obscured by the smooth contours associated with the rise in resistivity with depth.

Morrow (2007) investigated various possibilities to explain the change in resistivity structure from north to south along the beach (from Traverse 1 to 3), including possible changes in lithology and water extraction. Although borehole logs suggest that minor changes in lithology do occur, these do not correlate with the systematic changes in resistivity structure that are observed and are not, therefore, considered to be of significance. Similarly, differences in groundwater extraction from north to south are unlikely to be significant. It was concluded that the most likely cause of the change in geo-electric structure is the effect of the Waikanae Estuary (Fig. 2). Resistivity results obtained across the estuary by Morrow (2007), confirmed the earlier finding by Cozens (2003) that the sand beneath the estuary is saturated with saline water and has a resistivity of less than 2 Ωm down to nearly 20 m depth with resistivity remaining less than 10 Ωm to 30 m depth. This is similar to the resistivity structure observed below Traverse 1, and Morrow (2007) concluded that the gradual thinning of the very low resistivity surface layer southwards from Traverse 1 to Traverse 3 most probably reflects the change from conditions dominated by the influence of the estuary to conditions representative of the equilibrium of the saline interface with groundwater flow unaffected by the Waikanae River. Traverse 3, as the farthest from the estuary, was therefore selected for more detailed study.

4. Cross-borehole resistivity tomography

Three 10 m long vertical strings of electrodes, referred to as A–C were installed, as indicated in Fig. 3c, so as to straddle the inferred saline interface or mixing zone on Traverse 3 (Morrow, 2007). Each electrode string consisted of multicore cable with takeouts from separate internal wires at 1 m intervals. The takeout wires were terminated with spade terminals which were bolted to the actual electrodes made of marine grade stainless steel discs, 5 cm in diameter and 0.5 cm thick. The boreholes were drilled used a Kubota tractor-mounted drill rig, and initially cased with 80 mm internal diameter steel pipe. With the pipe in place an electrode string was lowered into the hole after which the casing was removed. Each hole was then filled, and left to stabilise and equilibrate for a week before any measurements were taken.

The electrode strings were installed 10 m apart in a straight line from the base of the coastal dunes to the top of the mean inter-tidal swash zone. The vertical separation of electrodes on each string was 1 m, with the upper electrode in each of Strings A and C 1.3 m below ground level, and that in String B at a depth of 1.7 m. Three monitoring boreholes which were used for measurement of water conductivity and water level were also installed, 2 m to the north of each of the electrode strings. The locations of the electrode strings and the vertical separation of the electrodes were chosen so as to give better resolution of the dynamics of the saline interface than could be achieved with the resistivity traverses. The only previously reported such measurements on a beach-face, those of Turner and Acworth (2004), utilized four electrode strings each horizontally separated by 5 m, and of 3 m in length.

Cross-borehole resistivity measurements, again using an ABEM resistivity meter and manual electrode switching system, were
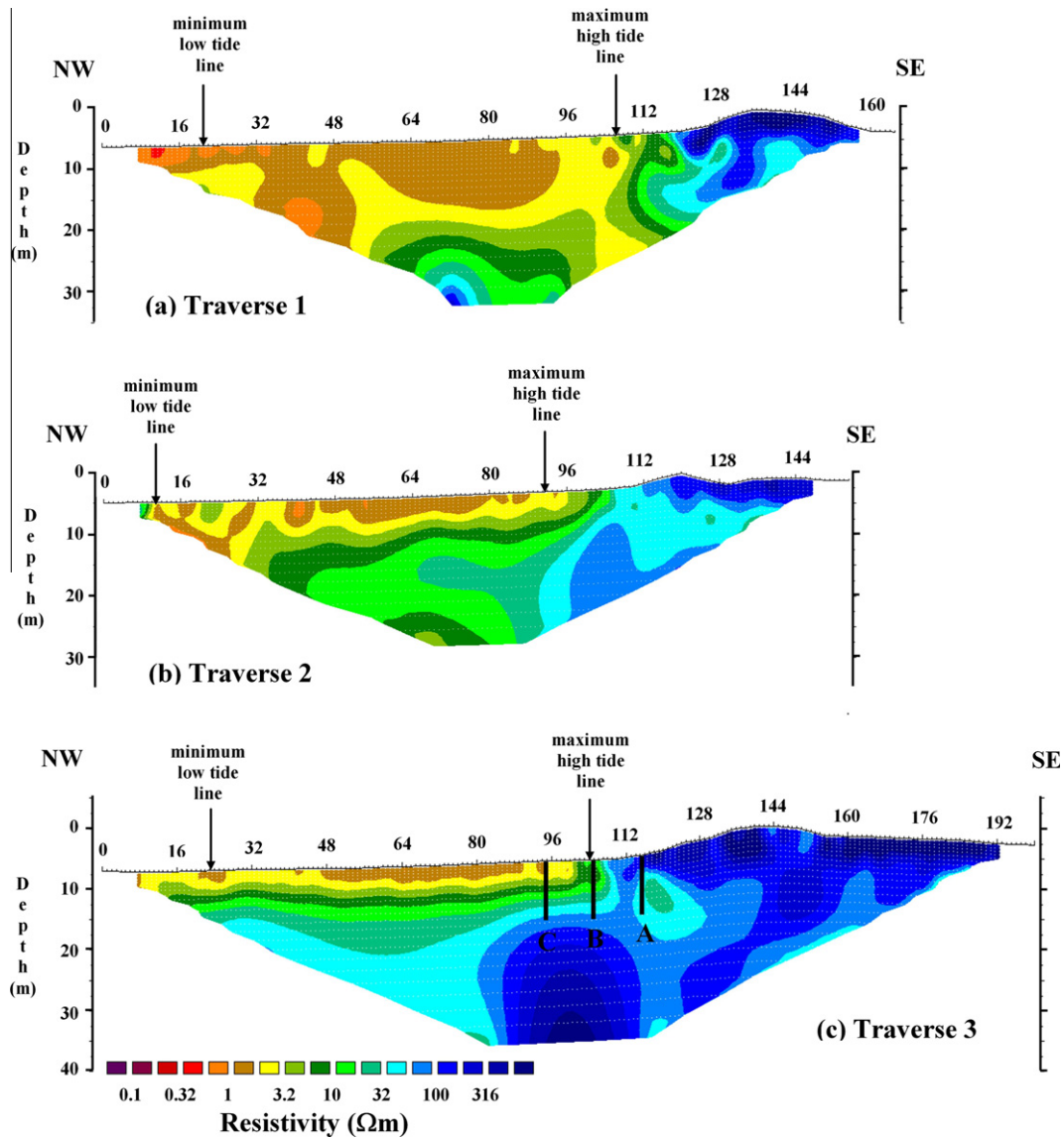
Fig. 3. 2-D resistivity models derived for the 3 resistivity traverses. Distances and depths are both in m. A, B and C on Traverse 3 show the locations of the three borehole electrode strings.

made between different combinations of the electrode strings at various times during the tidal cycle. In all cases the bipole–bipole configuration was used i.e. current was injected into, and removed from, the subsurface through electrodes in different boreholes, with the potential difference also being measured between electrodes in different boreholes. Although this configuration has potentially lower resolution than the dipole–dipole configuration (in which both current electrodes are in one borehole and both potential electrodes in another) it gives superior signal strength. This was regarded as important in a low resistivity environment in which potential differences were likely to be small.

A summary of the CRT measurements is given in Table 1. Each sequence of measurements took between 2 and 3 h to complete, timed to cover the tidal maximum or minimum. Each data set was inverted using Res2dinv, with differences in the surface elevation of the electrode strings included. Data from the low and high tidal cycles on 15 and 16 March 2007 were subsequently combined to derive resistivity models covering all three electrode strings. On both of these days the tidal range was similar (1.7 m compared to 2.1 m) and inversions of the combined datasets show little difference from those of the individual days. The resistivity structure

Table 1
Summary of cross-borehole resistivity measurements made on Paraparaumu Beach.

Date	Between electrode strings	Low or high tide	Period of measurements	Time of tide	Amplitude of tide
15.3.07	C & B	Low	12:10–15:50	13:30	1.7
15.3.07	C & B	High	18:00–21:00	19:39	1.7
16.3.07	B & A	High	07:30–10:10	08:10	2.1
16.3.07	B & A	Low	13:15–15:30	14:28	2.2
20.3.07	C & B	High	09:05–11:45	10:08	3.8
20.3.07	C & B	Low	15:00–17:15	16:27	3.8

thus derived for low tide, covering all three electrode strings, is shown in Fig. 4a. The structure derived from the data measured at high tide is shown in Fig. 4b.

The two resistivity structures shown in Fig. 4a and b are remarkably similar and contain no significant differences. This is perhaps not surprising as, for the tidal range sampled by these data, high tide barely reached electrode string C, the farthest down the beach. Nevertheless, the results show the detail of the resistivity structure to be considerably more complex than can be inferred
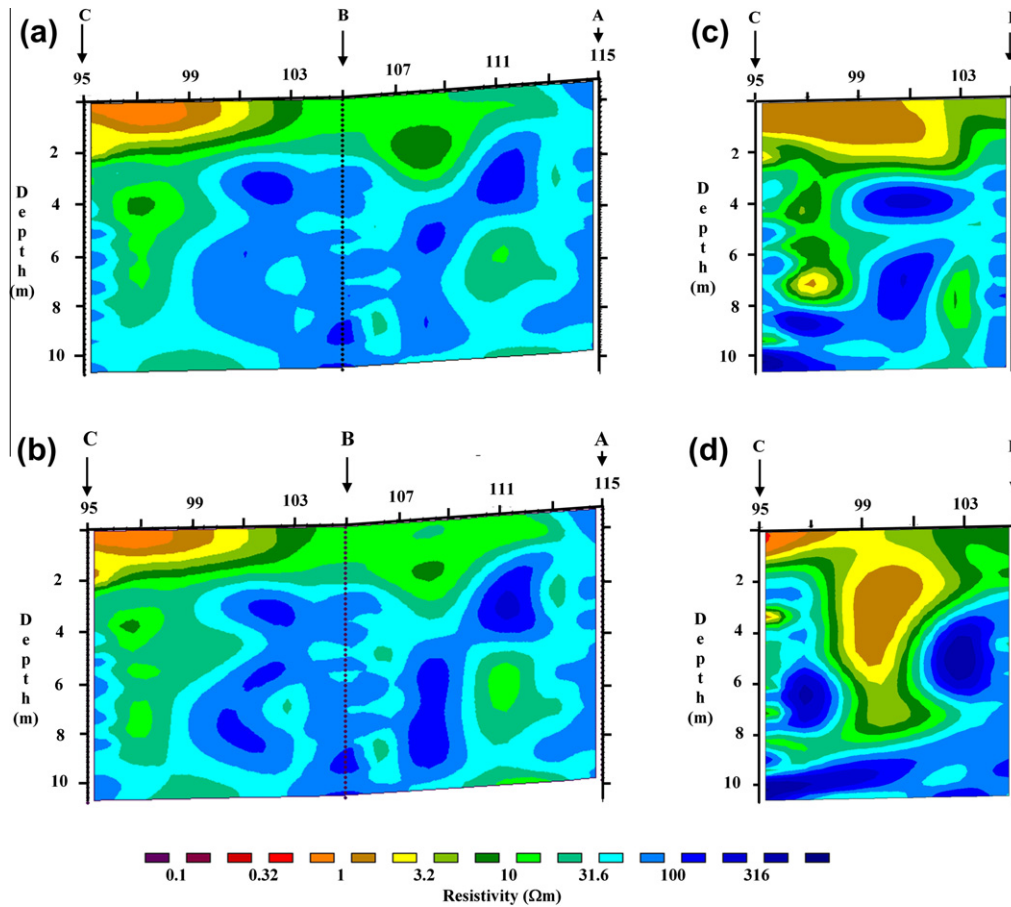
Fig. 4. 2-D models of resistivity structure derived from cross-borehole resistivity measurements on Traverse 3. (a) Model derived from measurements made over low tides on 15/16 March 2007 when the tidal range was ∼2 m. (b) Model derived from measurements made over high tides on the same days. (c) Model derived from measurements made over low tide on 20 March 2007 when the tidal range of 3.8 m. (d) Model derived from measurements made over high tide on the same date. Horizontal distances are in m from the W end of Traverse 3 corresponding to the scale shown in Fig. 3.

from the traversing results. Although the very low surface resistivity extends inland to approximately 100 m on the horizontal scale, comparable with the extent of this zone indicated by Traverse 3 (Fig. 3c), the thickness of the zone is much better resolved by the borehole data, as approximately 2 m. A similar horizontal layering and thickness of low resistivity on a beach face was also observed by Turner and Acworth (2004). Beneath this very low resistivity zone, a tongue of lower resistivity (∼10 Ωm) extends down to a depth of nearly 9 m, just inland of electrode string C. There is no indication of this feature in the resistivity model derived for Traverse 3. It is also clear from the borehole results that slightly higher, but still low, near-surface resistivity of around 10 Ωm extends almost as far inland as the base of the dunes, with a resistivity of less than 30 Ωm penetrating to ∼9 m depth close to electrode string A. Around borehole B, below 2–3 m depth, higher resistivity of the order of 50–100 Ωm is observed. Overall the cross-borehole results suggest that the model derived from the resistivity traverse, including for example the region of resistivity of order 30 Ωm seen inland of electrode string A in Fig. 3c, is in fact a significantly smoothed version of a much more varied and complex resistivity structure associated with the mixing zone of the saline interface.

Although it can be inferred that the resistivity structures shown in Fig. 4a and b cover the actual mixing zone, any effects due to tidal action are not apparent in these results. Consequently, as the resistivity models were derived from measurements taken over a relatively small tidal range, measurements between electrode strings B and C were repeated over a tidal cycle with a much great-

er range. Strings B and C were chosen because, as the two arrays furthest down the beach, it was assumed that any tidal influence would be greater in this area. A set of measurements were made during a tidal cycle with a range of 3.8 m on 20 March 2007. This range is just less than the maximum experienced at Paraparaumu Beach and during this particular tidal cycle, low tide went out further than on any other occasion when measurements were taken. During high tide the wave run-up went 3 m past electrode string B. The effect of this larger tidal range on the resistivity structure between strings B and C is shown in Fig. 4c and d. The basic geo-electric model for the area between electrode strings C and B at low tide during this large tidal cycle is similar to that shown in Fig. 4a and b with a layer of very low resistivity occurring within the top 2 m, and a region of resistivity of ∼10 Ωm penetrating to a depth of 8 m. However, there are now significant differences between the model derived from the low tide data and that derived from the measurements made at high tide. During high tide the low resistivity region deepens and expands considerably to become the dominant feature of the resistivity model. Variations in the location of regions of higher resistivity also testify to significant movement of water beneath the swash zone both vertically and horizontally, leading to the mixing of pockets of more or less saline water. This suggests that the area of mixing is in fact affected by the tidal variation, and also possibly through wave run-up as saline water infiltrates through the sand to greater depth, presumably taking paths dictated by minor variations in porosity and permeability.
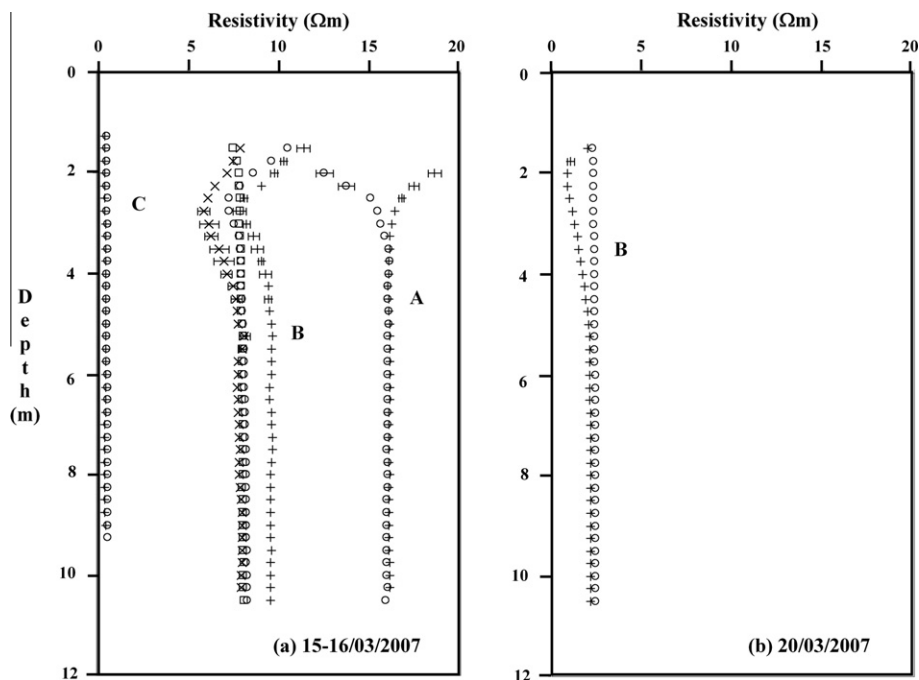
Fig. 5. Measurements of fluid resistivity as a function of depth in the three monitoring bores adjacent to electrode strings A–C. Circles/squares represent measurements made at high tide, crosses are measurements made at low tide. (a) Measurements made over the period 15–16 March 2007 over a tidal range of ~2 m. (b) Measurements made on 20 March 2007 over a tidal range of 3.8 m.

5. Fluid conductivity

A better understanding of the resistivity models shown in Figs. 3c and 4 can be obtained by considering fluid conductivity measurements made in conjunction with the cross-borehole measurements. Measurements of the conductivity of the pore fluid were made in the parallel monitoring bores. A conductivity (resistivity) profile was created by lowering a conductivity probe down a bore and taking conductivity measurements at 25 cm intervals until the bottom of the bore was reached. The meter was held at each successive depth for two minutes to obtain a stable reading. With a sample interval of 15 s, this allowed eight measurements to be taken at each depth increment. The average and standard deviations of each set of 8 readings for the tidal cycles corresponding to the resistivity models in Fig. 4 are shown in Fig. 5. As for the cross-borehole resistivity data, measurements were made covering both low and high tides.

It is clear that there is a significant variation in fluid resistivity over the 20 m range of the beach that is covered by the three boreholes. Borehole C, the closest to the sea, shows extremely low fluid resistivity, of ~0.5 Ωm, throughout the entire depth range. This is about twice the expected resistivity of seawater and indicates that borehole C can be inferred to be very close to the seaward boundary of the mixing zone. This inference is supported by the lack of variation in fluid resistivity between high and low tides. From the resistivity model of Figs. 3c it is impossible to deduce the bulk resistivity close to the location of borehole (electrode string) C beneath the near-surface low resistivity zone, as at the appropriate depths the model is dominated by the smooth contour variation from 3 to ~50 Ωm. The cross-borehole resistivity models (Fig. 4), however, suggest that the bulk resistivity at depths down to at least 8 m, just inland from borehole C, is about 10 Ωm. This increase in resistivity beneath the near-surface layer, while the observed fluid resistivity is constant, is most likely the result of a reduction in porosity resulting from increased compaction with depth. It should also be noted that the somewhat higher values

immediately adjacent to the electrode string are unrepresentative due to the disturbance caused by installation of the electrode strings – a feature also noted by Turner and Acworth (2004).

In borehole B, there is an offset in fluid resistivity values measured over low tide on 15/03/07 compared to the other measurements. There is also considerable variation in the observed fluid resistivity in the upper 4 m of the borehole. The offset may result from significant rainfall, which had occurred over the few days prior to measurements being taken, leading to a dilution of salinity. This then increased to more normal levels through subsequent tidal cycles. Coupled with this, the variations in the upper part of the borehole may also reflect the effect of tidal run-up percolating downwards. Apart from these shallow variations, the resistivity is again essentially constant over the entire depth range with an average value of about 8 Ωm. The observed fluid resistivity in borehole A is ~16 Ωm and, below 3 m in depth again shows no variation between high and low tides. Variations in the upper 3 m between measurements at high and low tides probably reflect the effects of wave run-up.

Fluid conductivity measurements made in borehole B over the larger tidal cycle corresponding to the resistivity models shown in Fig. 4c and d are shown in Fig. 5b. Although, in the near-surface, variations in fluid resistivity with depth are still apparent, the most significant feature is that the deeper, essentially constant, fluid resistivity is around 2 Ωm – only 25% of the value observed in borehole B for the previous measurements.

6. Discussion

In relation to the first objective of this study, as has been demonstrated in previous studies, resistivity traversing has proved to be a useful technique for locating the saline interface. The results show that the location and apparent shape of the saline interface on Paraparaumu Beach changes with distance from the Waikanae River and estuary. The major differences in the derived resistivity

structures (Fig. 3) show a significant increase in resistivity below about 15–20 m depth, with distance south of the estuary. This can be interpreted in terms of an increased thickness of the coastal wedge of sand close to the river mouth, which thins to the south. Thus, at a distance of only 400 m south of the river mouth (Traverse 1), the most significant variation in resistivity is that which occurs at the base of the coastal sand dunes. This has a shape which reflects the classic shape of a saline interface predicted by the Ghyben–Herzberg relationship. Beneath Traverse 2, 400 m further south of the river mouth, higher resistivity (10–30 Ωm) exists beneath the swash zone and is presumably related to a thinning of the sand wedge. In association with this the horizontal variation in resistivity at the base of the dunes is less marked. A further 400 m south (Traverse 3), the resistivity beneath the swash zone rises to 30–50 Ωm at 20 m depth, but resolution is lost due to the accumulation of contours. However, a horizontal variation in resistivity still occurs at the base of the dunes in the upper 20 m.

Wilson et al. (2006) used resistivity traversing to examine the saline interface on Te Horo beach, some 15 km to the north (Fig. 1), and concluded from the shape of the interface that, as a result of local groundwater extraction, saline intrusion had penetrated some 30 m towards the township. No such dramatic inference can be drawn from the resistivity traversing models derived for the present study. Nevertheless there are indications from all three traverses that, in the upper 20 m, some saline mixing is taking place beneath the coastal dunes ahead of the main transition zone from salt to fresh water. On all three traverses this takes the form of an area of resistivity of around 30–50 Ωm.

The results of the CRT yield a much more detailed picture of the saline interface beneath Traverse 3. The surface low resistivity region, also observed by Turner and Acworth (2004), is seen to be confined to the upper 2–3 m and is underlain by a region of much more variable resistivity which is related to the zone of mixing of saline and fresh water. This is emphasised by more detailed consideration of the observed fluid resistivity. Fluid resistivity is directly related on a log–log scale to the concentration of dissolved salts in the fluid. It is therefore possible, to a reasonable approximation, to express

$$\log(\rho_f) = A - \log(S)$$

where ρ_f is fluid resistivity, S is the concentration of dissolved salts, and A is a constant. Thus a factor of 10 change in concentration reduces the fluid resistivity by a factor of 10. As the measured fluid resistivity in borehole C (0.5 Ωm) is about twice that of pure seawater (0.25 Ωm) it implies that at the location of borehole C there is approximately 50% mixing of fresh and saline water. Similarly in borehole A the observed fluid resistivity of 16 Ωm suggests a 1–2% mixing of saline water with fresh water. For such a degree of mixing the observed bulk resistivity of around 30–50 Ωm seen in both Figs. 3c and 4 is consistent with that seen for a similar degree of mixing inferred by Wilson et al. (2006).

The ratio of bulk resistivity to fluid resistivity is referred to as the formation factor. At Te Horo, some 15 km to the north (Fig. 1) and in a broadly similar hydrogeological environment, Wilson et al. (2006) estimated the formation factor for the unconfined aquifer to be 2.6–2.9. Assuming that this value also applies to this study, the observed fluid resistivities in boreholes B and A imply bulk resistivities of approximately 25 and 50 Ωm respectively. Observed bulk resistivities in both Figs. 3c and 4 are in general agreement with these values. Similarly the observed fluid resistivity of 0.5 Ωm in borehole C predicts a bulk resistivity of ~1.5 Ωm, which is in agreement with the observed value in the upper 2–3 m of Figs. 3c and 4. Below these depths, as indicated earlier, correlation of the predicted value with the observed value is difficult because

of the steep gradient in the contours in Fig. 3c and localised effects adjacent to the actual borehole in Fig. 4.

The invariance over the tidal cycle of the fluid resistivity values measured below about 3 m depth in boreholes A and C suggests that these boreholes lie close to the margins of the main mixing zone which marks the saline interface. This implies that borehole B is positioned more or less in the middle of the mixing zone as was initially inferred from Fig. 3c. Thus the variations in both the fluid resistivity in borehole B, and the CRT images can be assumed to be the result of the dynamic processes occurring in the mixing zone.

Previous work on the response of the saline interface to tidal fluctuations (Inouchi et al., 1990; Ataie-Ashtiani et al., 1999; Wang and Tsay, 2001; Turner and Acworth, 2004; Cartwright et al., 2004; Kim et al., 2006; Acworth et al., 2007) has suggested that tides are observed to have three main possible effects on the saline interface: cause seawater to intrude inland as the hydraulic head rises and falls with the tide (Osborne, 2006); widen the zone of dispersion of saline water (Ataie-Ashtiani et al., 1999); and cause seawater to infiltrate directly from wave run-up (Turner and Acworth, 2004). The latter effect, which is intensified if the slope of the beach is flatter (Ataie-Ashtiani et al., 1999), is a likely contributor to the difference in resistivity structure between high and low tides seen in Fig. 4c and d, and the shallow variations in fluid resistivity observed in both boreholes A and B in Fig. 5. However, the deeper variations in fluid resistivity in borehole B suggest that the rising and falling tidal head also influences the mixing zone. In particular, the observation that higher fluid resistivity, following significant rainfall, is initially reduced by subsequent tidal action, and subsequently reduced further as the tidal range increases, suggests significant temporal variations in salinity occur within the mixing zone. These can be envisaged as a horizontal movement of near vertical salinity contours in response to, first, increased flow of fresh water towards the coast following rainfall, and, subsequently, landward movement of saline fluid into the mixing zone due to tidal variations in sea level. Assuming a linear horizontal variation in salinity between boreholes B and C, when the fluid resistivity is ~10 Ωm in borehole B a salinity corresponding to a resistivity of 2 Ωm occurs at about 97 m on the horizontal scale shown in Fig. 4. The occurrence of a fluid resistivity of 2 Ωm in borehole B during high spring tides therefore suggests a horizontal movement of at least 7–8 m of fluid within the mixing zone and a variation in the degree of mixing at borehole B from 2–3% sea water to ~13%. The horizontal range is consistent with the observed changes in bulk resistivity over a horizontal scale of about 5 m seen in Fig. 4c and d. The absence of more significant differences between the CRT models may well relate to fact that the length of time (2–4 h) required to collect the necessary data is a significant fraction of the tidal cycle (Table 1).

It appears therefore that the dynamics of the saline interface are influenced by both seawater infiltration from wave run-up and changes in tidal level. Turner and Acworth (2004) pointed out that changes in the saline interface were more noticeable when moving from neap to spring tides, or during a major storm event when wave run-up was greater. The observed difference between resistivity images taken over different tidal ranges supports this assertion. In contrast, the constancy of the fluid resistivity below 3 m depth in boreholes A and C suggests that there is no observable widening of the mixing zone in response to the tidal cycle.

These observations are highly relevant to the potential response of the saline interface to climate change and any consequent increase in sea level. Notwithstanding the inability in this study to resolve movement of the mixing zone as a whole during the tidal cycle, an increase in sea level will clearly lead to the establishment of a new dynamic equilibrium in which the mixing zone moves further inland. The first indications of such movement may well be

the result of penetration of wave run-up allowing penetration of saline water into the region beneath a new swash zone established further inland. Climatic changes that may lead to reduced freshwater discharge into the sea will exacerbate such changes. To address the extent to which this may occur in specific situations, future work should consider monitoring changes in the saline interface and mixing zone between wet and dry times of the year when there are significant changes in both abstraction and recharge of the aquifer.

Although it concentrates on a specific unconfined coastal aquifer in New Zealand the study demonstrates techniques and features which will be applicable to similar aquifers elsewhere. The ability of resistivity traversing to image the saline interface has been demonstrated previously. However, it is now clearly shown that CRT has the potential to yield much higher resolution images of this zone as well as to provide information on the mixing of saline and fresh water, particularly if sufficient hydrological data are available to allow comparative quantitative hydrogeological modelling of the saline interface.

Acknowledgements

References

Acworth, R.I., Dasey, G.R., 2003. Mapping of the hyporheic zone around a tidal creek using a combination of borehole logging, borehole electrical tomography and cross-creek electrical imaging, New South Wales, Australia. Hydrogeology Journal 11, 368–377.

Acworth, R.I., Hughes, C.E., Turner, I.L., 2007. A radioisotope tracer investigation to determine the direction of groundwater movement adjacent to a tidal creek during spring and neap tides. Hydrogeology Journal 15, 281–296.

Albouy, Y., Andrieux, P., Rakotondrasoa, G., Ritz, M., Descloitres, M., Join, J.-L., Rasolomanana, E., 2001. Mapping coastal aquifers by joint inversion of DC and TEM soundings – three case histories. Ground Water 39, 87–97.

Ataie-Ashtiani, B., Volker, R.E., Lockington, D.A., 1999. Tidal effects on sea water intrusion in unconfined aquifers. Journal of Hydrology 216, 17–31.

Batayneh, A.T., 2006. Use of electrical resistivity methods for detecting subsurface fresh and saline water and delineating their interfacial configuration: a case study of the eastern dead sea coastal aquifers, Jordan. Hydrogeology Journal 14, 1277–1283.

Bauer, P., Supper, R., Zimmermann, S., Kinzelbach, W., 2006. Geoelectric imaging of groundwater salinization in the Okavango Delta, Botswana. Journal of Applied Geophysics 60, 126–141.

Cartwright, N., Li, L., Nielsen, P., 2004. Response of the salt–freshwater interface in a coastal aquifer to a wave induced groundwater pulse: field observation and modelling. Advances in Water Resources 27, 297–303.

Choudhury, K., Saha, D.K., Chakraborty, P., 2001. Geophysical study for saline water intrusion in a coastal alluvial terrain. Journal of Applied Geophysics 46, 189–200.

Cozens, N., 2003. Resistivity Investigations of Groundwater in the Vicinity of the Waikanae River Mouth. Unpublished BSc (Hons) Dissertation, School of Earth Sciences, Victoria University of Wellington, Wellington, 51p.

Daniels, J.J., 1977. Three-dimensional resistivity and induced polarisation modeling using buried electrodes. Geophysics 42, 1006–1019.

de Groot-Hedlin, C., Constable, S., 1990. Occam's inversion to generate smooth, two-dimensional models from magnetotelluric data. Geophysics 55, 1613–1624.

Duque, C., Calvache, M.L., Pedrera, A., Martin-Rosales, W., Lopez-Chicano, M., 2008. Combined time domain electromagnetic soundings and gravimetry to determine marine intrusion in a detrital coastal aquifer (Southern Spain). Journal of Hydrology 349, 536–547.

Ebraheem, A.-A.M., Senosy, M.M., Dahab, K.A., 1997. Geoelectrical and hydrochemical studies for delineating ground-water contamination due to salt-water intrusion in the northern part of the Nile delta, Egypt. Ground Water 35, 216–222.

Goldman, M.M., Gilad, D., Ronen, A., Melloul, A., 1991. Mapping of seawater intrusion into the coastal aquifer of Israel by the time domain electromagnetic method. Geoexploration 28, 153–174.

Harkness, M.D., 2004. Hydrology of the Waikanae River. Report prepared for the Kapiti Coast District Council by Opus International Consultants, Wellington, 32p.

Ingham, M., McConchie, J.A., Wilson, S.R., Cozens, N., 2006. Measurement and monitoring of saline intrusion using dc resistivity traversing. Journal of Hydrology (NZ) 45, 89–102.

International Association of Hydrologists, 2003. Groundwater – from development to management. Briefing paper for 3rd World Water Forum, Kyoto, Japan, March 2003.

Inouchi, K., Kishi, Y., Kakinuma, T., 1990. The motion of coastal groundwater in response to the tide. Journal of Hydrology 115, 165–191.

Johannesson, J.K., Rapley, B., 1961. The ground waters of the Waikanae–Paraparaumu Region. New Zealand Journal of Science 4, 443–452.

Jones, A., Gyopari, M., 2005. Investigating the sustainable use of shallow groundwater on the Kapiti Coast. Greater Wellington Regional Council, 51p.

Kim, K.-Y., Seong, H., Kim, T., Park, K.-H., Woo, N.-C., Park, Y.-S., Koh, G.-W., Park, W.-B., 2006. Tidal effects on variations of fresh-saltwater interface and groundwater flow in a multilayered coastal aquifer on a volcanic island (Jeju Island, Korea). Journal of Hydrology 330, 525–542.

Koukadaki, M.A., Karatzas, G.P., Papadopoulou, M.P., Vafidis, A., 2007. Identification of the saline zone in a coastal aquifer using electrical tomography data and simulation. Water Resources Management 21, 1881–1898.

Looms, M.C., Jensen, K.H., Binley, A., Nielsen, L., 2008. Monitoring unsaturated flow and transport using cross-borehole geophysical methods. Vadose Zone Journal 7, 227–237.

Morrow, F.J., 2007. Dynamics of the saline interface of the shallow unconfined aquifer at Kapiti. Unpublished MSc thesis, School of Earth Sciences, Victoria University of Wellington. Wellington, 126p.

Osborne, A.M., 2006. Movement of water within the Waikanae Shallow Gravel Aquifer and its Interaction with the Waikanae River. Unpublished MSc thesis, School of Geography, Environmental and Earth Sciences, Victoria University of Wellington, Wellington, 165p.

Reynolds, T.I., 1992. Kapiti Coast sub-region – Groundwater Review. Publication No: WRC/CI-T/92/44. Wellington, New Zealand, Greater Wellington Regional Council.

Ruehe, Y., 2004. Assessing groundwater recharge on the Kapiti coast using a water balance model. Unpublished BSc (Hons) Dissertation, School of Earth Sciences, Victoria University of Wellington, Wellington, 62p.

Sasaki, Y., 1992. Resolution of resistivity tomography inferred from numerical simulation. Geophysical Prospecting 40, 453–464.

Shima, H., 1992. 2D and 3D resistivity and image reconstruction using cross-hole data. Geophysics 55, 682–694.

Slater, L., Binley, A.M., Daily, W., Johnson, R., 2000. Cross-hole electrical imaging of a controlled saline tracer injection. Journal of Applied Geophysics 44, 85–102.

Turner, I.L., Acworth, R.I., 2004. Field measurements of beachface salinity structure using cross-borehole resistivity imaging. Journal of Coastal Research 20, 753–760.

URS, 2003. Waikanae/Otaihanga Borefield Drilling Strategy. KCDC Contract 401. Prepared for Kapiti Coast District Council, URS, Wellington, 24p.

URS, 2004a. Waikanae Borefield. Assessment of Environmental Effects. URS, Wellington, 91p.

URS, 2004b. Waikanae Borefield Technical Report. Prepared for Kapiti Coast District Council, Wellington, 57p.

Wang, J., Tsay, T.-K., 2001. Tidal effects on groundwater motions. Transport in Porous Media 43, 159–178.

Welch, C., 2004. Groundwater recharge from the Waikanae River. Unpublished BSc (Hons) Dissertation, School of Earth Sciences, Victoria University of Wellington, Wellington, 62p.

Wellington Regional Council, 1992. Kapiti Coast District Water Resource Study – Water Resource Statement, vol. 2. Wellington Regional Council, Wellington.

Wellington Regional Council, 1994. Hydrology of the Kapiti Coast. WRC/CI-T/G-94/13. Wellington Regional Council, Wellington, New Zealand, 211p.

Wellington Regional Council, 2000. Paraparaumu Shallow Groundwater Investigation. Publication number WRC/RINV-T-00/27. Wellington Regional Council.

White, P.A., 1985. Handbook on hydro geological applications of earth resistivity measurements. In: Water and Soils Publication No. 90. Water and Soil Directorate. Ministry of Works and Development, New Zealand, p. 41.

White, P.A., 2001. Groundwater resources in New Zealand. In: Rosen, M., White, P. (Eds.), Groundwaters of New Zealand, pp. 45–75.

Wilson, S.R., 2003. The saltwater–freshwater interface. Te Horo Beach, Kapiti Coast. Unpublished MSc thesis, School of Earth Sciences, Victoria University of Wellington, Wellington, 145p.

Wilson, S.R., Ingham, M., McConchie, J.A., 2006. The applicability of earth resistivity methods for saline interface definition. Journal of Hydrology 316, 301–312.